Original Article

Bone regeneration of mouse critical-sized calvarial defects with human mesenchymal stem cell sheets co-expressing BMP2 and VEGF

Tingting Guo [a,b], Xiaohong Yuan [c], Xin Li [d], Yi Liu [b,e*], Jian Zhou [f**]

[a] Department of General Dentistry and Emergency Dental Care, Beijing Stomatological Hospital, Capital Medical University, Beijing, PR China
[b] Laboratory of Tissue Regeneration and Immunology and Department of Periodontics, Beijing Key Laboratory of Tooth Regeneration and Function Reconstruction, School of Stomatology, Capital Medical University, Beijing, PR China
[c] Department of Pathology, Beijing Stomatological Hospital, Capital Medical University, Beijing, PR China
[d] Department of Preventive Dentistry, Beijing Stomatological Hospital, Capital Medical University, Beijing, PR China
[e] Immunology Research Center for Oral and Systemic Health, Beijing Friendship Hospital, Capital Medical University, Beijing, PR China
[f] Department of VIP Dental Service, Beijing Key Laboratory of Tooth Regeneration and Function Reconstruction, School of Stomatology, Capital Medical University, Beijing, PR China

Background/purpose: Over-dependence on existing synthetic scaffolds and insufficient osteoinductive and vasculogenic growth factors have limited the development of bone regeneration. The study aimed to assess the feasibility of using marrow-derived mesenchymal stem cells (BMSCs) cell sheets co-expressing bone morphogenetic proteins 2 (BMP2) and vascular endothelial growth factor (VEGF) for repairing critical-sized calvarial defects.

 * Corresponding author. Laboratory of Tissue Regeneration and Immunology and Department of Periodontics, Beijing Key Laboratory of Tooth Regeneration and Function Reconstruction, School of Stomatology, Capital Medical University, Tian Tan Xi Li No. 4, Beijing 100050, PR China.
 ** Corresponding author. Department of VIP Dental Service, Beijing Key Laboratory of Tooth Regeneration and Function Reconstruction, School of Stomatology, Capital Medical University, Tian Tan Xi Li No. 4, Beijing 100050, PR China.
 E-mail addresses: lililiuyi@163.com (Y. Liu), zhoujian@ccmu.edu.cn (J. Zhou).

Critical size bone defect; BMP2 and VEGF

Materials and methods: BMSCs cell sheets were genetically engineered to express BMP2/VEGF alone or together. Alterations in osteogenic markers were examined by quantitative real-time PCR (qRT-PCR) and western blotting. A critical-sized calvarial bone defect model was used to investigate the osteogenesis effects of BMP2/VEGF cell sheets alone or in combination. The efficacy was assessed with micro-computed tomography (micro-CT) and histology.

Results: In vitro, the expression of BMP2 and VEGF through lentiviral transduction was confirmed by qRT-PCR and western blotting against BMP2 and VEGF. Lentiviral delivery of BMP2 and VEGF resulted in the upregulation of osteogenic markers. In vivo, in a critical-sized calvarial bone defect model, 3D-reconstructed micro-CT images revealed that treatment of the calvarial defects with the BMP2/VEGF cell sheet resulted in significantly greater amounts of newly formed bone at 8 weeks after surgery than treatment with cell sheets with single gene transduction or vehicle controls. The results were confirmed by histological assessment by H&E staining and Masson staining.

Conclusion: This study demonstrates that BMP2/VEGF co-expressing BMSCs sheets promote bone regeneration in critical-sized calvarial bone defects. The BMP2/VEGF cell sheets provide a functional bioactive scaffold for critical-size bone reconstruction.

Introduction

Traditional stem cell-based bone tissue engineering strategies use a synthetic biomaterial scaffold seeded with regenerative cells and growth factors to induce healing via intramembranous ossification.[1]

However, undesirable issues associated with this synthetic scaffold-based approach for bone regeneration have hindered clinical implementation, such as cell loss, small quantities of seeded cells, low cell adhesion efficiency, and unequal cell distribution.[2] The delivery of a sufficient number of stem cells with osteogenic and angiogenic activity to the defect area is the first step in ensuring the clinical feasibility of a stem cell-based treatment. In addition, the presence of synthetic materials may significantly interfere with cell–cell interactions, which are essential for tissue development.[3] Furthermore, interactions between the scaffold and stem cells may alter cell phenotypes.[4] Synchronizing scaffold degradation with new tissue formation at defect sites is also challenging. If synchrony is not correctly achieved, cell proliferation, extracellular matrix (ECM) production, remodeling, and construct integration can be inhibited, thus ultimately compromising the integrity of the newly formed bone.[5]

Depending on the type of scaffold, chemicals used for scaffold production and degradation byproducts may result in cytotoxicity and immunogenicity.[6] Moreover, this combination of synthetic scaffolds and stem cells has not produced the desired results, owing to cell necrosis at the bulk of the scaffold, associated with nutrient diffusion and insufficient oxygen.[7] Cell sheet engineering has been developed as a unique, scaffold-free method of tissue regeneration, which provides the advantages of maintenance of ECM and cell–cell junctions without the impairments induced by biomaterials and their degradation.[8]

Angiogenesis and mineralization are coupled during bone repair.[9] Angiogenesis is a critical initial step during bone repair that re-establishes the blood supply to deliver oxygen, nutrients, and cells. Because both bone morphogenetic proteins 2 (BMP2) and vascular endothelial growth factor (VEGF) are involved in osteoinduction and angiogenesis and synergistically promote bone formation, combined delivery of these two factors has been suggested to lead to better outcomes in bone regeneration than delivery of either factor alone.[10,11] The drawbacks of using growth factors, such as poor stability and short half-lives, have limited clinical application. Through a convergence of gene therapy and bone engineering over the past decade, genetically engineered cells can now continually produce functional proteins that promote bone formation.[12]

This study prepared a genetically modified bone marrow-derived mesenchymal stem cells (BMSCs) sheet through the dual lentiviral transduction of BMP2 and VEGF genes into BMSCs. We obtained the cell sheets as a scaffold-free device and studied their osteogenic properties in vitro and their effects on bone formation in vivo. To evaluate bone regeneration ability, we used micro-computed tomography (micro-CT) to measure the new bone volume, then performed a histomorphometric evaluation to evaluate the microscopic structure of the newly formed bone. The modified BMSCs sheets are expected to serve as a scaffold-free alternative to repair critical-sized bone defects.

Materials and methods

Study animals

Nine-week-old female C57BL/6J mice were purchased from Vital River Laboratory Animal Technology Co., Ltd., Beijing, China. The animals were housed in separate pathogen-free

facilities under controlled temperature (25 °C) and photo-periods (12:12-h light: dark cycle), and were fed a standard diet and tap water. The mice were acclimated to these conditions for 7 days before the experiment. This study was conducted according to the guidelines of the Animal Ethics Committee of the School of Stomatology, Capital Medical University (Beijing, China). All animal experiments were performed under the institutionally approved protocols for the use of animals in research (Capital Medical University No. KQYY-201907-003).

Lentiviral vector construction and transduction of BMSCs

Self-inactivation lentiviral vector carrying the coding sequences of VEGF (reference sequence: NM_001025368.2) for the VEGF group; BMP2 (reference sequence: NM_001200.3) for the BMP2 group; and BMP2 (reference sequence: NM_001200.3):IRES:VEGF (reference sequence: NM_001025368.2) for the B−V group were purchased from VectorBuilder Inc., Guaugzhou, China. A gene encoding enhanced green fluorescent protein (EGFP) was used as a lentiviral infection marker. A lentiviral vector carrying only the EGFP coding sequence served as a control (NULL group). BMSCs in early passages (passages 2 or 3) were infected in monolayer culture with the indicated lentiviruses (multiplicity of infection = 30) to attain 80—90% infection efficiency, as confirmed by fluorescence microscopy. Polybrene (VectorBuilder Inc.) at 5 μg/ml was added to improve the transduction efficiency. Puromycin (Invitrogen Corp., San Diego, CA, USA) at 1 μg/ml was used for drug-resistance marker selection.

Construction of mesenchymal stem cell sheets

A total of 1.0×10^6 hBMSCs (Beijing Donghuafang Biotechnology Co., Beijing, China, product code HUXMA-01001, Long-bone marrow mesenchymal stem cells, p2) were subcultured in 60 mm dishes. Ascorbic acid (Sigma—Aldrich Corp., St. Louis, MO, USA) was added at 20.0 μg/ml to the culture medium for the duration of the experiment, as previously reported.[13] The cells became confluent after 2—3 days. Confluent cells were cultured for 10—14 days until the cell layer began to fold on itself at the edges of the dishes, thus indicating that cell sheets had formed and could be detached.

RNA preparation and expression analysis by quantitative real-time PCR (qRT-PCR)

Total RNA was extracted from BMSCs with TRIzol reagent (Thermo Fisher Technology (China) Co., Ltd, Shanghai, China) according to the manufacturer's instructions (Thermo Fisher Technology (China) Co., Ltd). Then 2 μg aliquots of RNA were synthesized with random hexamers or oligo (dT) and reverse transcriptase through real-time PCR. The reactions were performed with a QuantiTect SYBR Green PCR kit (QIAGEN China (Shanghai) Co., Ltd., Shanghai, China) and an IcycleriQ Multi-color Real-time PCR Detection System. The amplification primer sequences are shown in Table 1.

Table 1 Sequences of primers used in the present study.

Primer ID	Sequence(5'-3')
RUNX2_forward	AGGGACTATGGCGTCAAACA
RUNX2_revserse	GGCTCACGTCGCTCATCTT
β-actin_forward	CGGTTCCGATGCCCTGAGGCTCT
β-actin_revserse	CGTCACACTTCATGATGGAATA
ALP_forward	GGACAGGACACACACACACA
ALP_revserse	CAAACAGGAGAGCCACTTCA
OPN_forward	CCAATCGTCCCTACAGTCGA
OPN_revserse	ACTCACCGCTCTTCATGTGA
VEGFA_forward	TGGTGGACATCTTCCAGGAG
VEGFA_revserse	GGA AGCTCATCTCTCCTATGTG
BMP2_forward	GCTGATCATCTGAACTCCACT
BMP2_revserse	CGTCAAGGTACAGCATCGAGAT
GAPDH_forward	GACTCATGACCACAGTCCATG
GAPDH_reverse	TCAGCTCAGGGATGACCTTG

RUNX2= runt-related transcription factor 2, ALP= alkaline phosphatase; OPN= osteopontin, BMP2= bone morphogenetic proteins 2; VEGF=vascular endothelial growth factor, GAPDH=glyceraldehyde-3-phosphate.

Western blot analysis

Total protein was extracted with RIPA buffer (10 mM Tris—HCl, 1 mM EDTA, 1% sodium dodecyl sulfate, 1% Nonidet P-40, 1:100 proteinase inhibitor cocktail, 50 mM β-glycerophosphate, and 50 mM sodium fluoride). The samples were separated on a 10% sodium dodecyl sulfate-polyacrylamide gel (Applygen Technologies Inc., Beijing, China) and transferred to PVDF membranes (Millipore Corporation, Billerica, MA, USA). The membranes were blocked with 5% nonfat milk for 1 h and incubated with primary antibodies at 4 °C overnight. This was followed by incubation with HRP-conjugated anti-mouse or anti-rabbit IgG (1:10000; Abcam, San Francisco, CA, USA) for 1 h at room temperature. Blots were visualized with Immobilon Western Chemiluminescent HRP Substrate (Millipore Corporation). Antibodies to the following were used in this work: runt-related transcription factor 2 (RUNX2; Abcam), osteopontin (OPN; Abcam), heat shock protein 90 (HSP90; Sigma—Aldrich Corp., St.), alkaline phosphatase (ALP; BioLegend, San Diego, CA, USA), bone morphogenetic protein 2 (BMP2; ABclonal Technology Co., Ltd., Wuhan, China), and vascular endothelial growth factor (VEGF; Biosynthesis Biotechnology Co., Ltd., Beijing, China).

Critical-sized calvarial bone defect model

C57BL/6J (10-week-old female) mice were administered 1% chloral hydrate (0.04 ml/g body weight) intraperitoneally. The skin was prepared, and the operation area was disinfected with iodophor. A sagittal incision was created on the scalp to the middle sagittal crest, and the periosteum was dissected bluntly. A critical-sized defect (4 mm diameter with full-thickness) was made at the center of the dorsal calvarium with a surgical drilling unit and a trephine.[14] The calvarial disk was removed, and the cell sheets were implanted within the defect. The surface was covered with a Bio-Guide grafting membrane, which

exceeded the bone defect range by approximately 2 mm. The defect sites were closed with an interrupted silk suture (Fig. 1). After the surgery, the animals were housed in soft-bedded cages and given free access to food and water.

A virus containing the EGFP sequence without target gene sequences served as the negative control (NULL group). Defects without cell sheets served as a control (BLANK group).

At 8 weeks after transplantation, all animals were sacrificed, and the samples were harvested and fixed with 4% paraformaldehyde. The samples were sectioned and stained with hematoxylin and eosin (H&E), and Masson's trichrome.

Micro-computed tomography (micro-CT) analysis of the bone formation

The samples harvested at 8 weeks were scanned with a Siemens Inveon CT (Siemens Inveon, Berlin, Germany) instrument with a voltage of 80 kV, an electric current of 500 mA, exposure time of 2000 ms, and a pixel resolution of 15 μm with a 0.5 mm aluminum filter to visualize the volume of mineralized tissue. The projection image was reconstructed in Inveon Research Workplace V2.2.0 software. The quantitative analyses were performed in Materialise Mimics V17.0 and Geomagic Studio 2013. Critical-sized defects with 4 mm diameter and full-thickness in height were determined according to the region of interest. The new bone volume was calculated.

Statistical analysis

Statistics was calculated in SPSS 23.0 statistical software. The student's t-test was used to determine statistical significance. A value of $P < 0.05$ was considered statistically significant. All values are described as the mean ± standard deviation (SD).

Results

BMP2 and VEGF lentiviral expression upregulates BMP2 and VEGF mRNA and protein levels

The transduction of BMSCs with EGFP, BMP2, VEGF, and BMP2+VEGF viral particles was efficient (80−90%), and the transduced cells demonstrated similar spindle-shaped morphology in monoculture (Fig. 2A−E). Compared with the NULL and BMP2 groups, the VEGF and B−V groups had significantly higher VEGF mRNA and VEGF protein expression on days 7 and 14 (Fig. 2F and G) after viral infection. Similarly, significantly higher levels of BMP2 mRNA and secreted BMP2 protein were observed in the BMP2 and B−V groups than in the NULL and VEGF groups on days 7 and 14 (Fig. 2E, G).

Lentiviral mediated combined delivery of BMP2 and VEGF upregulates osteogenic markers in vitro

The expression levels of osteogenic markers, including ALP, RUNX2, and OPN, were examined to evaluate osteoblast differentiation in each group on days 7 and 14.

Compared with those in the NULL group, BMSCs overexpressing BMP2 showed significantly higher mRNA levels of *ALP* (Fig. 3A; $P < 0.05$), *RUNX2* (Fig. 3B; $P < 0.05$), and *OPN* (Fig. 3C; $P < 0.001$). Only the expression of *OPN* (Fig. 3C; $P < 0.001$) was markedly higher in the VEGF group. In addition, the most notable changes in the expression of *RUNX2* (Fig. 3B; $P < 0.05$) and OPN (Fig. 3C; $P < 0.001$) were observed in the B−V group. However, there was no statistically significant difference in *ALP* expression between the
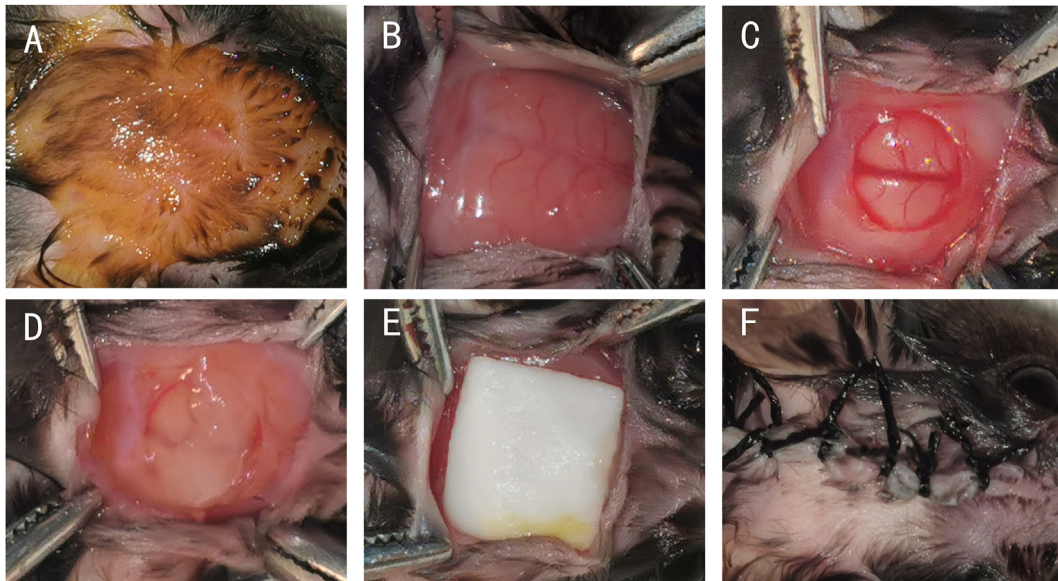

Figure 1 Critical-sized calvarial bone defect model. A, Skin preservation and sterilization. B, Incision. C, Critical-sized defects 4 mm in diameter with full thickness, prepared with a trephine. D, Implanted cell sheet. E, Surface covered with Bio-Guide. F, Suture.
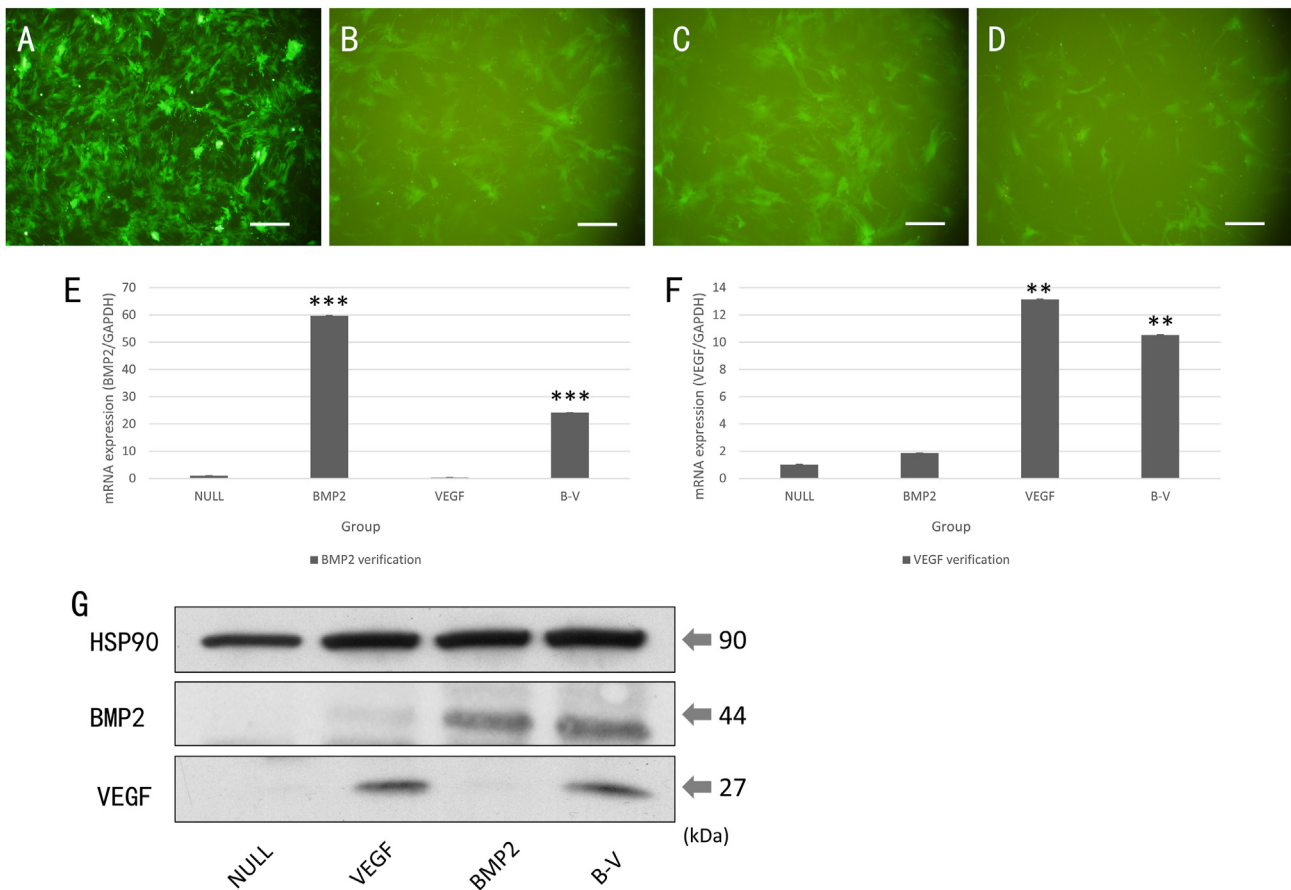
Figure 2 BMP2 and VEGF lentiviral vectors upregulate the expression of BMP2 and VEGF, respectively, in BMSCs. Expression of EGFP in BMSCs after lentiviral vectors transduction for 48 h, observed under an inverted fluorescence microscope. A, NULL group. B, BMP2 group. C, VEGF group. D, B−V group. The bar in the figure indicates 500 μm. E, F, mRNA expression of *BMP2* and *VEGF* in each group on day 7. G, Protein expression of BMP2 and VEGF in each group on day 14. BMSCs transduced with BMP2 and B−V secreted large quantities of BMP2. Similarly, significant upregulation of VEGF levels was found in both VEGF and B−V groups. *BMP2* and *VEGF* mRNA levels were normalized to the *GAPDH* mRNA level. BMP2 and VEGF protein levels were normalized to the HSP90 level. Student's t-test was used to determine statistical significance. The data shown represent the means $\pm$ SD (n = 3). ***$P < 0.001$, **$P < 0.01$, compared with the NULL group.

VEGF and B−V groups and the NULL group. Moreover, similar gene expression of *RUNX2* was found in the VEGF and the NULL groups.

As indicated in Fig. 3D and E, the expression levels of ALP, RUNX2, and OPN, which are important markers of osteogenic differentiation, were higher in all groups than in the NULL group. Additionally, the osteogenic markers ALP, RUNX2, and OPN were significantly induced in the B−V group compared with the BPM2 and VEGF alone groups. Therefore, these data indicated that lentiviral-mediated delivery of BMP2 and VEGF alone or in combination upregulated osteogenic markers in vitro.

Fabrication of cell sheets

After culturing for 14 days, the high-density BMSCs formed a thick, sturdy cell sheet, which was easily detached with a cell scraper and handled with forceps (Fig. 4A). The cell sheet was folded into a small ball for transplantation (Fig. 4B).

Histological evaluation of newly formed bone after 4 and 8 weeks

After surgical implantation of the cell sheets, no animals showed any signs of inflammation or infection induced by the Bio-Guide grafting membrane or BMSCs. Decalcified sections were stained with H&E and Masson's trichrome to evaluate the morphology of the regenerated tissue.

The histological results revealed greater new bone formation in the B−V, BMP2, and VEGF groups than in the BLANK and NULL groups. Figs. 5 and 6 show representative histological sections of the five experimental groups at 4 and 8 weeks after surgery. At both time points, only traces of new bone were embedded in cell-rich, fibrous connective tissue spanning the defects in the BLANK and NULL group (Fig. 5A−F, Fig. 6B, C, F, G). In the BMP2 group, moderate new bone formation was seen at both time points. New tissue in the defect comprised osteoid and woven bone surrounded by osteoblast cells. Lacunae-embedded osteocytes were observed, and several more
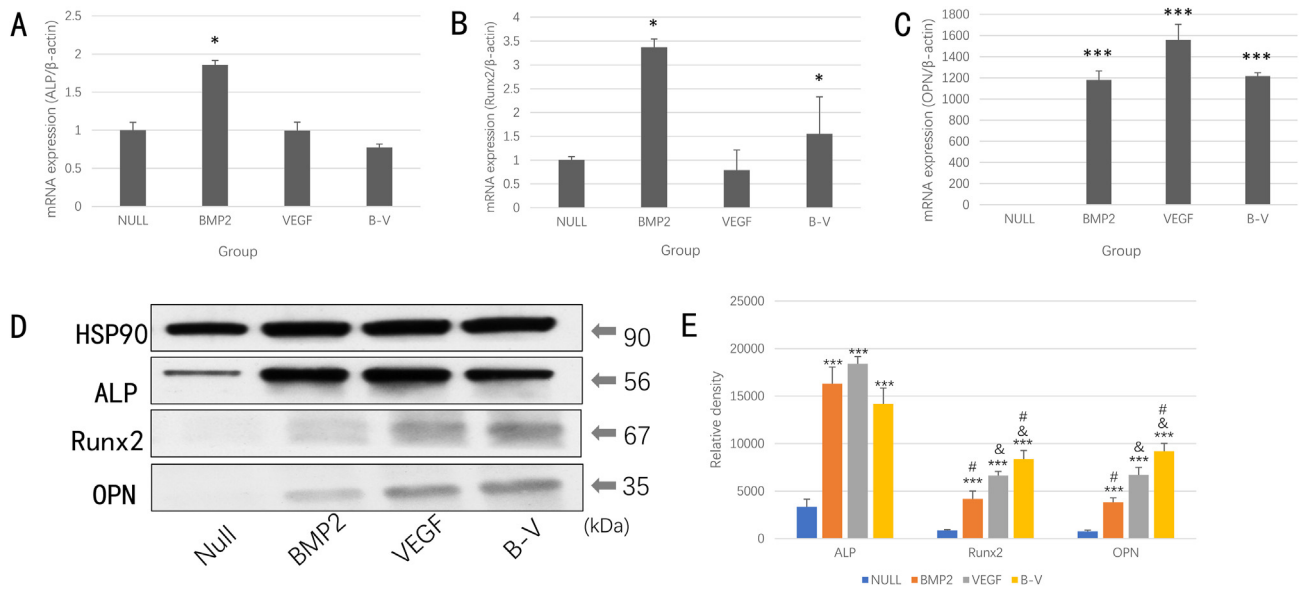
Figure 3 Lentiviral combined delivery of BMP2 and VEGF is associated with the upregulation of osteogenic markers. mRNA and protein expression of osteogenesis-associated genes in vitro at days 7 and 14. A, ALP. B, RUNX2. C, OPN. Significantly higher mRNA levels of *ALP*, *RUNX2*, and *OPN* were found in the BMP2 group. The expression of *OPN* was markedly higher in the VEGF group. Notable changes in expression of *RUNX2* and *OPN* were observed in the B—V group. D, E, Protein expression of osteogenesis-associated genes in vitro at day 14. ALP, RUNX2, and OPN increased in all groups, in contrast to the NULL group. ALP, RUNX2, and OPN were highly induced in the B—V group, in contrast to the BPM2 and VEGF groups. mRNA levels were normalized to the β-actin mRNA level. Protein levels were normalized to the HSP90 level. Student's t-test was used to determine statistical significance. The data shown represent the means ± SD (n = 3). *P < 0.05, ***P < 0.001, compared with the NULL group. &P < 0.05, compared with the BPM2 group. #P < 0.05, compared with the VEGF group.
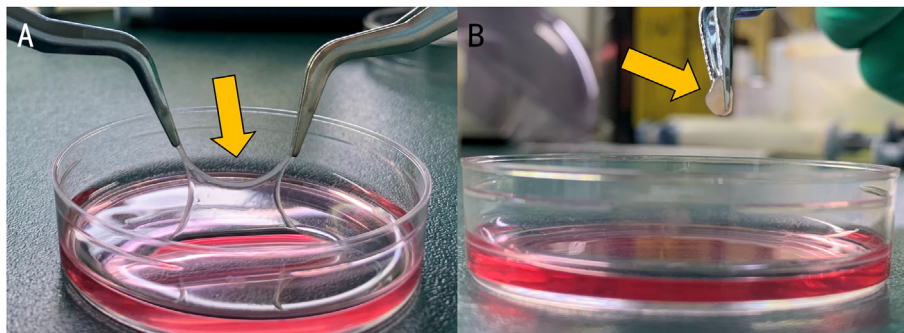

Figure 4 The cell sheet. A, The cell sheet can be handled with forceps (yellow arrow). B, The cell sheet is folded into a small ball for transplantation (yellow arrow).

mature lamellar structures with interspersed marrow-like tissue containing blood vessels were present (Fig. 5G—I, Fig. 6J and K). By week 4, the VEGF and B—V groups showed varying degrees of immature new bone formation (light blue) originating from the defect margin, surrounded by osteogenic cells (Fig. 5L, O). In addition, denser blood vessels were observed in both groups (Fig. 5K, N). At week 8, new bone tissue was more extensive in the B—V group than in all other groups, and abundant organized lamellar bone containing lacunae-embedded osteocytes was present (Fig. 6R, S).

Masson staining is associated with the molecular size of anionic dye and tissue permeability. Molecular size is reflected by molecular weight. Low molecular weight compounds easily penetrate dense structures with low tissue permeability, whereas high molecular weight compounds can only enter the porous and highly permeable tissues.[15] With bone maturation, collagen becomes arranged more regularly and densely, and the crosslinking increases, thus altering collagen staining.[16] According to this principle, the blue color indicates early new bone tissue, and the red color indicates mature bone tissue, thus enabling a comparison of the degree of maturation of the bone matrix and callus during bone repair.

At 8 weeks after surgery, a red collagen staining area was observed in the NULL group, BMP2 group, VEGF group, and B—V group. The red staining area in the BMP2, VEGF, and B—V groups was larger than that in the BLANK and NULL
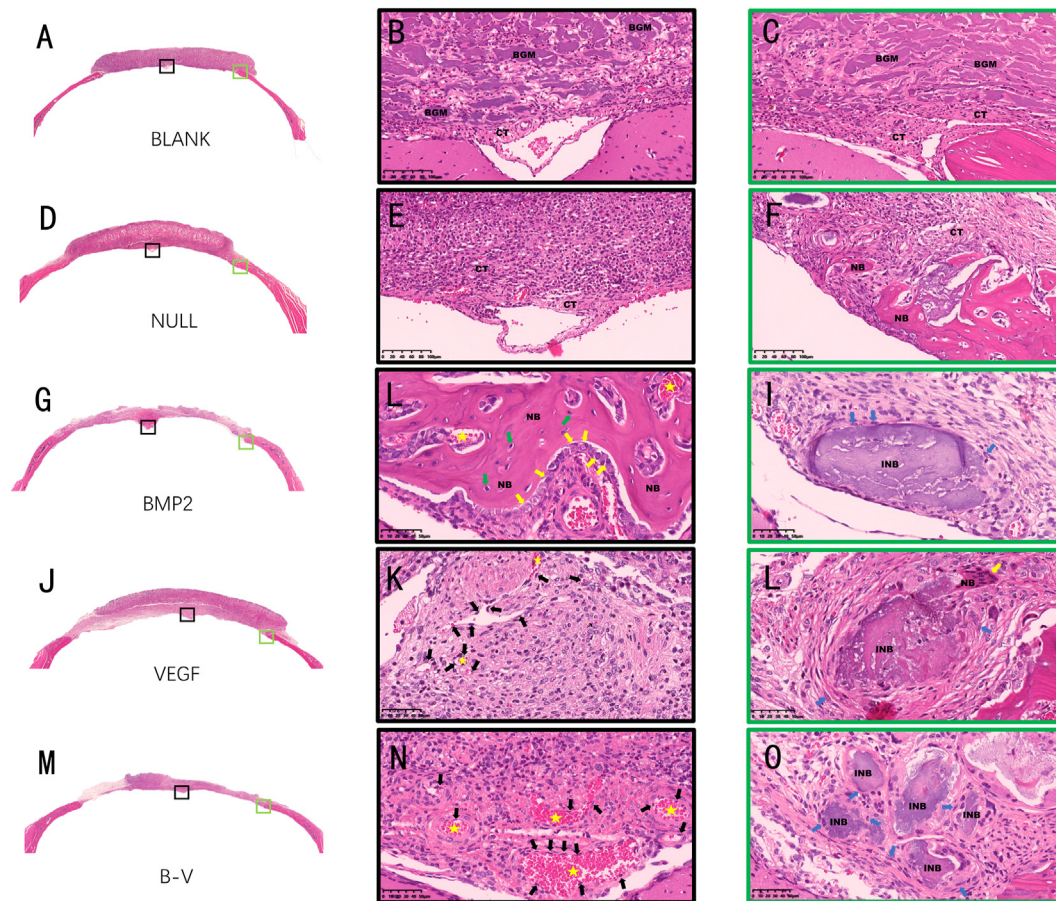
Figure 5 H&E stained images of bone defect regions at 4 weeks. A, D, G, J, M, H&E staining of the calvarial bone, showing the coronal calvarial defect with newly formed bone. B, E, L, K, N, H&E stained sections at a central region of the defect. C, F, I, L, O, H&E stained sections at the defect margin. 5A-F, Only mild new bone formation was embedded in connective tissue spanning the defects in the BLANK and NULL groups. 5G-I, Moderate new bone formation surrounded by osteoblasts (yellow arrows) was seen in the BPM2 group. Lacunae-embedded osteocytes (green arrows) were present. 5J-O, The VEGF and B—V groups showed varying degrees of immature new bone formation, seen in light blue, originating from the defect margin, surrounded by osteogenic cells (blue arrows). More frequent blood vessels (black arrows indicate vascular endothelial cells; yellow stars indicate erythrocytes) were observed (NB, new bone; BGM, Bio-Guide graft membrane; CT, connective tissue; INB, immature new bone).

groups. The ratio of the red staining area in the B—V group was significantly higher than that in any other group, thus suggesting that the B—V cell sheet produced more bone with a dense and crosslinked matrix. However, a similar ratio of red staining area was found in the BMP2 group and the VEGF group, thereby indicating no difference in bone maturity between these groups (Fig. 6D, H, L, P, T, W).

Accelerated healing of critical-sized calvarial defects by BMP2 and VEGF co-expressing cell sheet scaffold-free constructs

Tissue samples were collected for micro-CT after 8 weeks of healing. As shown in Fig. 6A, E, I, M, Q, V, the 3D-reconstructed micro-CT images of the bone defects revealed that the treatment of the calvarial defects in the B—V group (2.8925 ± 0.5780 mm^3) significantly improved the amount of newly formed bone 8 weeks after surgery, followed by the BMP2 and VEGF groups, as compared with the BLANK group and NULL group. Furthermore, the BMP2

group (2.17728 ± 0.29160 mm^3) showed more bony bridges than the VEGF group (1.88974 ± 0.65689 mm^3). The mean new bone volume in the NULL group (0.77296 ± 0.23663) was higher than that in the BLANK group (0.48424 ± 0.29228 mm^3) but was not statistically different.

Discussion

The critical size bone defect model is one of the most widely used models to detect the osteogenic potential of growth factors and scaffold materials using mesenchymal stem cells.[17] The current study assesses the feasibility of using cell sheets co-expressing BMP2 and VEGF to repair critical-sized calvarial defects. The results demonstrate that BMP2/VEGF co-expressing BMSCs sheets promote bone regeneration in critical-sized calvarial bone defects.

The use of scaffolds in combination with osteogenic cells has become the gold standard in bone tissue engineering strategies. However, conventional tissue engineering methods involving the seeding of cells into synthetic
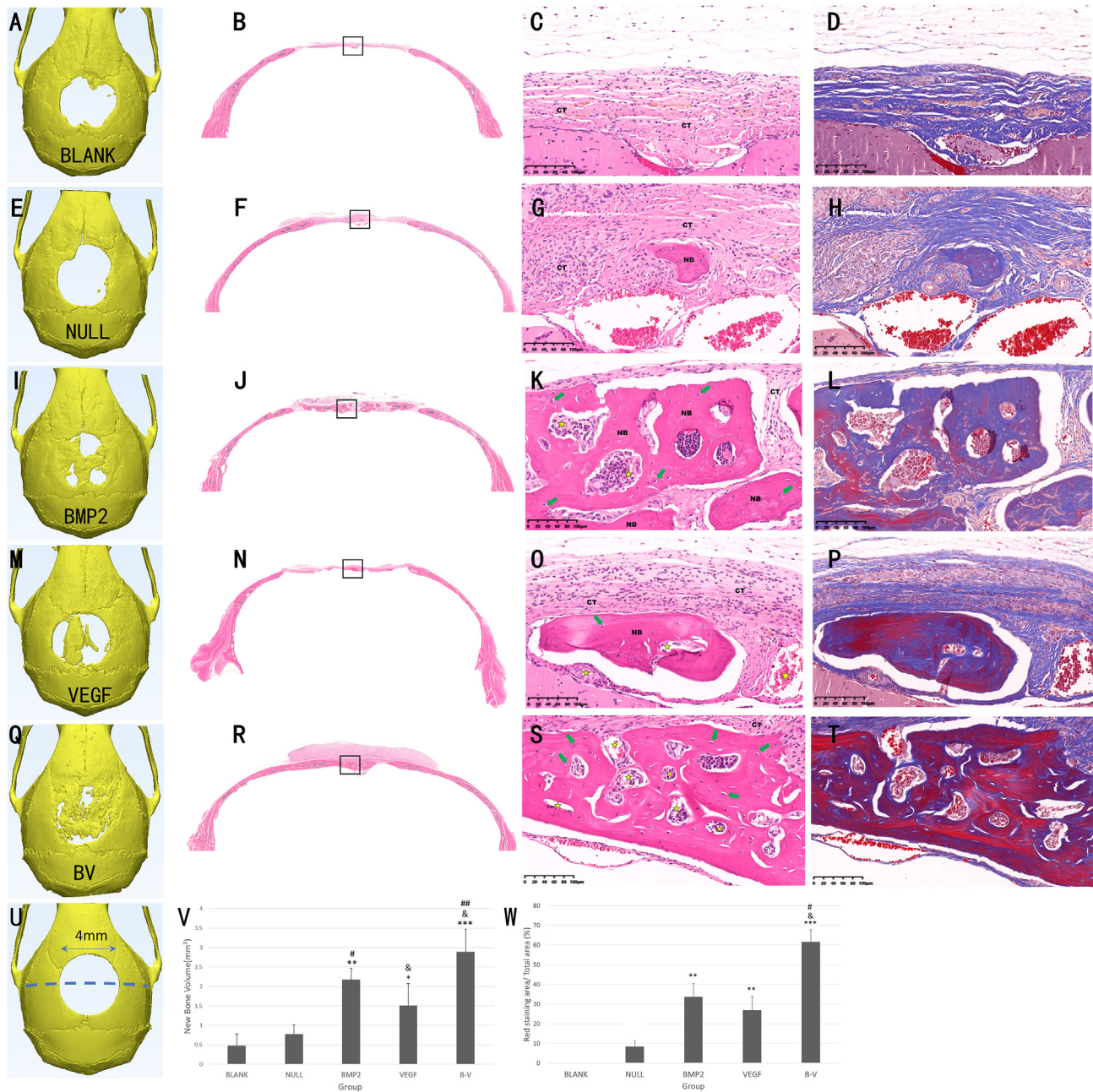
Figure 6 BMP2 and VEGF co-expressing BMSCs sheet scaffold-free constructs accelerate healing of critical-sized calvarial defects. 6A, E, I, M, Q, V, The 3D-reconstructed micro-CT images of the bone defects with newly formed bone. The B—V group showed significantly greater amounts of newly formed bone 8 weeks after surgery, followed by the BMP2 and VEGF groups, as compared with the BLANK or NULL groups. B, F, G, N, R, H&E staining of the calvarial bone, showing the coronal calvarial defect with newly formed bone. C, G, K, O, S, H&E staining magnified image. New bone tissue containing lacunae-embedded osteocytes (green arrows) was more extensive in the B—V group than all other groups. More frequent blood vessels (yellow stars indicate erythrocytes) were observed. D, H, L, P, T, Masson's trichrome staining. The red stained area in the BMP2, VEGF, and B—V groups was larger than that in the BLANK and NULL groups. The ratio of red stained area in the B—V group was significantly higher than that in all other groups. U, Schematic diagram illustrating the direction of the histological section. Student's t-test was used to determine statistical significance. The data shown represent the means ± SD (n = 3), *$P < 0.05$, **$P < 0.01$, ***$P < 0.001$, compared with the NULL group. &$P < 0.05$, compared with the BPM2 group. #$P < 0.05$, ##$P < 0.01$, compared with the VEGF group (NB, new bone; CT, connective tissue).

biodegradable scaffolds may present complications such as cell loss, small quantities of seeded cells, and inflammatory reactions with the degradation of the scaffolds.[2] Moreover, before scaffold materials are used in bone tissue reconstruction, the cells must be manipulated with proteolytic enzymes, such as trypsin or dispase, that degrade ECM

molecules and cell surface proteins, which play essential roles in forming the bone formation microenvironment.[18] Therefore, an alternative regeneration strategy was developed to overcome these disadvantages.

Cell sheets are layers of cells containing intact ECM and cell-surface proteins, such as growth factor receptors, ion channels, and cell−cell junction proteins. Most importantly, cell sheets and deposited ECM can be attached to host tissues with minimal loss of cells. Specifically, these cell sheets are based on hyperconfluent cells, forming extensive cell−cell interactions and synthesizing a substantial quantity of ECM.[19] In addition, cell sheets have high density and can be used as tissue engineering scaffolds to support cell growth. Researchers have attempted to exploit these characteristics to repair bone defects using cell sheets without scaffolds. Onishi et al. implanted cell sheets in a rat femoral non-union model. The results demonstrated that the cell sheets group had high osteoinductive and osteoconductive capacity.[20] The injection of osteogenic cell sheets into a rat femoral critical fracture healing model enhanced bone regeneration and finally led to the bone union.[21]

This study demonstrated that the BMP2 and VEGF co-expressing cell sheets robustly accelerated the healing of critical-sized calvarial defects. Micro-CT analysis indicated greater new bone formation in the B−V, BMP2, and VEGF groups than in the BLANK and NULL groups. As shown in Fig. 6A, E, I, M, Q, V, the 3D-reconstructed micro-CT images indicated that the B−V group showed a significant increase in the amount of newly formed bone 8 weeks after surgery, followed by the BMP2 and VEGF groups, as compared with the BLANK and NULL groups. The mean new bone volume in the NULL group was higher than that in the BLANK group but was not statistically different.

We observed unsatisfactory bone formation in the NULL group. We believe that the main reason for this finding was the absence of osteogenic factors and vascular networks in the central area of the critical-sized bone defects. Intramembranous bone formation fails in the absence of a network of blood vessels that deliver nutrients and growth factors to osteoblast and precursors. It has been reported in multiple studies that Poor blood supply impedes bone healing.[22] Consistently, implanting cell-seeded scaffolds that did not stimulate prompt vasculature has been reported to result in cell necrosis in the center of scaffolds.[23] Therefore, critical-sized bone defect repair can be challenging due to insufficient growth factors and blood vessel ingrowth.

Various growth factors have been clinically proved for their abilities to promote bone healing. In the present study, BMP2 and VEGF were selected as the most promising candidates. BMP2, a member of the transforming growth factor-β superfamily, is highly osteoinductive and promotes bone healing.[24] BMP2 induced bone formation is coupled with angiogenesis.[25] The highly coordinated process involves various growth factors and cytokines, including VEGF, promoting endothelial cell migration and proliferation.[26] BMP2 and VEGF reciprocally regulate each other's biological activity during bone repair. Therefore, delivery of BMP2 and VEGF in combination has been suggested for better healing of critical-size bone defects than only delivery of either factor alone.[27,28]

In the present study, BMP2 and VEGF BMSCs sheets were engineered through lentiviral transduction.

We tested the osteogenesis ability in vitro. The most notable changes in mRNA expression of *RUNX2* (Fig. 3B) and *OPN* (Fig. 3C) were found in the B−V group. Additionally, the osteogenic protein markers ALP, RUNX2, and OPN were highly induced in the B−V group (Fig. 3D and E). The experimental results confirmed that lentiviral-mediated delivery of BMP2 and VEGF in combination was associated with the up-regulation of specific osteogenic markers in vitro.

The BMP2 and VEGF co-expressing BMSCs sheet scaffold-free strategy to facilitate bone formation was then investigated in critical-sized bone defects in mice. The histological results revealed that new bone tissue was more extensive in the B−V group than in all other groups, with large organized lamellar bone containing lacunae-embedded osteocytes (Fig. 6R, S). Moreover, we used Masson staining to compare bone maturity. The ratio of the red staining area in the B−V group was significantly higher than that in all other groups, thus suggesting that the new bone was more mature (Fig. 6D, H, L, P, T, W). Together, our data indicated that the in vivo osteogenesis induced by BMP2 and VEGF in combination was superior to that induced by BMP2 alone or VEGF alone at the same time point.

This study demonstrates that a BMP2 and VEGF co-expressing BMSCs sheet scaffold-free based strategy promotes bone regeneration in critical-sized calvarial bone defects in mice. This finding implies that modified BMSCs sheets may offer an excellent alternative for craniofacial bone regeneration. Overall, our in vitro and in vivo observations serve as critical proof of concept for product development.

Declaration of competing interest

The authors have no conflicts of interest relevant to this article.

Acknowledgments

References

1. Meijer GJ, de Bruijn JD, Koole R, van Blitterswijk CA. Cell-based bone tissue engineering. *PLoS Med* 2007;4:e9.
2. Roseti L, Parisi V, Petretta M, et al. Scaffolds for bone tissue engineering: state of the art and new perspectives. *Mater Sci Eng C Mater Biol Appl* 2017;78:1246−62.

3. Chen SS, Fitzgerald W, Zimmerberg J, Kleinman HK, Margolis L. Cell-cell and cell-extracellular matrix interactions regulate embryonic stem cell differentiation. *Stem Cell* 2007;25:553—61.

4. Abarzúa-Illanes PN, Padilla C, Ramos A, et al. Improving myoblast differentiation on electrospun poly(ε-caprolactone) scaffolds. *J Biomed Mater Res* 2017;105:2241—51.

5. Lanza R, Langer R, eds. *Principles of tissue engineering*. Waltham: Elsevier, 2020.

6. Park JY, Park SH, Kim MG, Park S-H, Yoo TH, Kim MS. Biomimetic scaffolds for bone tissue engineering. In: Noh I, ed. *Biomimetic medical materials*. Singapore: Springer Singapore, 2018:109—21.

7. Uchihara Y, Akahane M, Okuda A, et al. Supplying osteogenesis to dead bone using an osteogenic matrix cell sheet. *J Orthop Sci* 2018;23:578—84.

8. Chen M, Xu Y, Zhang T, et al. Mesenchymal stem cell sheets: a new cell-based strategy for bone repair and regeneration. *Biotechnol Lett* 2019;41:305—18.

9. Diomede F, Marconi GD, Fonticoli L, et al. Functional relationship between osteogenesis and angiogenesis in tissue regeneration. *Int J Mol Sci* 2020;21:E3242.

10. Sharma S, Sapkota D, Xue Y, et al. Delivery of VEGFA in bone marrow stromal cells seeded in copolymer scaffold enhances angiogenesis, but is inadequate for osteogenesis as compared with the dual delivery of VEGFA and BMP2 in a subcutaneous mouse model. *Stem Cell Res Ther* 2018;9:23.

11. Zhang C, Meng C, Guan D, Ma F. BMP2 and VEGF165 transfection to bone marrow stromal stem cells regulate osteogenic potential in vitro. *Medicine (Baltim)* 2018;97:e9787.

12. Park SY, Kim KH, Kim S, Lee YM, Seol YJ. BMP-2 gene delivery-based bone regeneration in dentistry. *Pharmaceutics* 2019;11:393.

13. Wei F, Qu C, Song T, et al. Vitamin C treatment promotes mesenchymal stem cell sheet formation and tissue regeneration by elevating telomerase activity. *J Cell Physiol* 2012;227:3216—24.

14. Gupta DM, Kwan MD, Slater BJ, Wan DC, Longaker MT. Applications of an athymic nude mouse model of nonhealing critical-sized calvarial defects. *J Craniofac Surg* 2008;19:192—7.

15. Flint MH, Lyons MF, Meaney MF, Williams DE. The Masson staining of collagen—an explanation of an apparent paradox. *Histochem J* 1975;7:529—46.

16. Lim J, Lee J, Yun HS, Shin HI, Park EK. Comparison of bone regeneration rate in flat and long bone defects: calvarial and tibial bone. *Tissue Eng Regen Med* 2013;10:336—40.

17. Gomes PS, Fernandes MH. Rodent models in bone-related research: the relevance of calvarial defects in the assessment of bone regeneration strategies. *Lab Anim* 2011;45:14—24.

18. Gu R, Liu H, Zhu Y, Liu X, Wang S, Liu Y. Is extracellular matrix (ECM) a promising scaffold biomaterial for bone repair? *Histol Histopathol* 2021;36:1219—34.

19. Chen M, Xu Y, Zhang T, et al. Mesenchymal stem cell sheets: a new cell-based strategy for bone repair and regeneration. *Biotechnol Lett* 2019;41:305—18.

20. Onishi T, Shimizu T, Akahane M, et al. Osteogenic extracellular matrix sheet for bone tissue regeneration. *Eur Cell Mater* 2018;36:68—80.

21. Shimizu T, Akahane M, Morita Y, et al. The regeneration and augmentation of bone with injectable osteogenic cell sheet in a rat critical fracture healing model. *Injury* 2015;46:1457—64.

22. Hausman MR, Schaffler MB, Majeska RJ. Prevention of fracture healing in rats by an inhibitor of angiogenesis. *Bone* 2001;29:560—4.

23. Hao Z, Song Z, Huang J, et al. The scaffold microenvironment for stem cell based bone tissue engineering. *Biomater Sci* 2017;5:1382—92.

24. Riley EH, Lane JM, Urist MR, Lyons KM, Lieberman JR. Bone morphogenetic protein-2: biology and applications. *Clin Orthop Relat Res* 1996;324:39—46.

25. Schott NG, Friend NE, Stegemann JP. Coupling osteogenesis and vasculogenesis in engineered orthopedic tissues. *Tissue Eng B Rev* 2021;27:199—214.

26. Kim HY, Park JH, Kim MJ, Lee JH, Oh SH, Byun JH. The effects of VEGF-centered biomimetic delivery of growth factors on bone regeneration. *Biomater Sci* 2021;9:3675—91.

27. Simunovic F, Finkenzeller G. Vascularization strategies in bone tissue engineering. *Cells* 2021;10:1749.

28. Lee E, Ko JY, Kim J, Park JW, Lee S, Im GI. Osteogenesis and angiogenesis are simultaneously enhanced in BMP2-/VEGF-transfected adipose stem cells through activation of the YAP/TAZ signaling pathway. *Biomater Sci* 2019;7:4588—602.